

Connecting flavor at low- and high- p_T in the SMEFT

Olcyr Sumensari^{a,*}

^a*Université Paris-Saclay, CNRS/IN2P3, IJCLab, 91405 Orsay, France*

E-mail: olcyr.sumensari@ijclab.in2p3.fr

We discuss the high-energy probes of flavor physics operators in the $pp \rightarrow \ell\nu$ and $pp \rightarrow \ell\ell'$ processes, with $\ell, \ell' \in \{e, \mu, \tau\}$, and explore their complementarity with low-energy flavor measurements. We consider the Standard Model Effective Field Theory (SM EFT) as our framework and we discuss two explicit examples: (i) the discrepancies observed in the $b \rightarrow c\tau\nu$ transition, and (ii) the $b \rightarrow s\nu\bar{\nu}$ decays that are currently studied at Belle-II. We also briefly comment on the current status of the SM predictions for these low-energy observables.

*20th International Conference on B-Physics at Frontier Machines (Beauty2023)
3-7 July, 2023
Clermont-Ferrand, France*

*Speaker

1. Introduction

Flavor physics observables are powerful probes of physics beyond the Standard Model (SM) at low-energies, since they can be sensitive to energy scales well beyond the reach of the direct searches at the LHC. The most constraining of these observables are the ones related to rare processes, which are either suppressed or forbidden in the SM. Noticeable examples are Flavor Changing Neutral Current (FCNC) decays, which are suppressed by the loop and CKM factors in the SM, allowing us to probe scales as large as $O(10^5 \text{ TeV})$ [1]. Currently, there is an extensive experimental program dedicated to K -, D - and B -meson decays, which will offer many opportunities to unveil deviations from the SM predictions in precision measurements [2].

The precision frontier is one of the best options to seek new physics effects if the scale Λ where new physics particles arise is very large. However, flavor data is also compatible with concrete flavor-physics scenarios with a much lower scale Λ , in the $O(\text{TeV})$ range, provided flavor violation is suppressed, as realized e.g. in Minimal Flavor Violation [3] and scenarios with the $U(2)^5$ flavor symmetry [4]. This is particularly relevant to reconcile flavor observables with other SM issues such as the hierarchy problem that points at new physics at the TeV scale. In these scenarios, the direct and indirect searches at the LHC are also useful probes of new physics in the flavor sector, as we discuss in these proceedings.

Under the assumption that new physics arises well above the electroweak scale, the SM Effective Field Theory (SMEFT) provides the best description of experimental data [5]. Over the past several years, the high-energy tails of the $pp \rightarrow \ell\nu$ and $pp \rightarrow \ell\ell'$ processes (with $\ell, \ell' \in \{e, \mu, \tau\}$) have shown to be complementary to the flavor-physics measurements at low-energies, see Ref. [6, 7] and references therein. These observables allow us to probe semileptonic operators with five quark flavors that are available in the proton, with contributions that are energy-enhanced in the tails of the kinematical distributions [8]. An example of this complementarity is the discrepancy between the SM predictions and the experimental determinations of the ratios $R_{D^{(*)}} = \mathcal{B}(B \rightarrow D^{(*)}\tau\nu)/\mathcal{B}(B \rightarrow D^{(*)}l\nu)$ [9], with $l \in \{e, \mu\}$, for which LHC is essential to discard several proposed new physics explanations [6].

In the following, we will explore this complementarity between low- and high-energy probes in B -physics observables. In Sec. 2 and 3, we will briefly review the EFT description of $pp \rightarrow \ell\nu$ and $pp \rightarrow \ell\ell'$ at high-energies. These results will then be used in Sec. 4 to discuss two few specific examples: (i) the $R_{D^{(*)}}$ ratios and (ii) the decays based on the $b \rightarrow s\nu\nu$ transition, which are related through $SU(2)_L \times U(1)_Y$ gauge invariance.

2. EFT framework

We assume that the new physics scale lies well above the electroweak scale and consider the EFT invariant under the $SU(3)_c \times SU(2)_L \times U(1)_Y$ gauge symmetry, namely the SMEFT [5]. The leading effects in the SMEFT are described by $d = 6$ operators.

$$\mathcal{L}_{\text{eff}}^{(6)} = \sum_a \frac{C_a^{(6)}}{\Lambda^2} \mathcal{O}_a^{(6)}, \quad (1)$$

where Λ denotes the EFT cutoff. The effective coefficients are generically denoted by $C_a^{(6)}$ and the operators $\mathcal{O}_a^{(6)}$ can be of several types. We will consider the Warsaw basis for the $d = 6$ operators [5]

ψ^4	Operator	ψ^4	Operator +h.c.
$O_{lq}^{(1)}$	$(\bar{l}\gamma^\mu l)(\bar{q}\gamma_\mu q)$	O_{ledq}	$(\bar{l}^a e)(\bar{d}q^a)$
$O_{lq}^{(3)}$	$(\bar{l}\gamma^\mu \tau^I l)(\bar{q}\gamma_\mu \tau^I q)$	$O_{lequ}^{(1)}$	$(\bar{l}^a e)\varepsilon_{ab}(\bar{q}^b u)$
O_{lu}	$(\bar{l}\gamma^\mu l)(\bar{u}\gamma_\mu u)$	$O_{lequ}^{(3)}$	$(\bar{l}^a \sigma^{\mu\nu} e)\varepsilon_{ab}(\bar{q}^b \sigma_{\mu\nu} u)$
O_{ld}	$(\bar{l}\gamma^\mu l)(\bar{d}\gamma_\mu d)$		
O_{eq}	$(\bar{e}\gamma^\mu e)(\bar{q}\gamma_\mu q)$		
O_{eu}	$(\bar{e}\gamma^\mu e)(\bar{u}\gamma_\mu u)$		
O_{ed}	$(\bar{e}\gamma^\mu e)(\bar{d}\gamma_\mu d)$		

Table 1: Hermitian (left) and non-Hermitian (right) dimension $d = 6$ semileptonic operators in the SM EFT. Quark and lepton doublets are denoted by q and l , respectively, and the weak singlets read u , d and e . $SU(2)_L$ indices are denoted by a, b , with $\varepsilon_{12} = -\varepsilon_{21} = +1$, and $SU(3)_c$ indices are omitted. Flavor indices are also omitted in this Table.

and focus on the ones that contribute at tree level to Drell-Yan processes. There are only three types of operators that fulfill this requirement: (i) four-fermion semileptonic operators (ψ^4), (ii) dipole operators ($\psi^2 H X$), and (iii) Higgs-current operators ($\psi^2 H^2 D$).

The Higgs-current operators contribute to the partonic processes $q\bar{q} \rightarrow \ell\ell'$ via the modification of the W - and Z -boson couplings to SM fermions and, therefore, cannot induce an energy-enhancement of the amplitude. The contributions from the dipoles to the amplitude \mathcal{M} scale as $\mathcal{M} \propto vE/\Lambda^2$, whereas the one from semileptonic operator scale as $\mathcal{M} \propto E^2/\Lambda^2$, which can be prominent at the tails of the distributions [6]. In the following, we will focus on the semileptonic operators defined in Table 1, as they provide the largest contributions to the observables that we consider.

3. Probing flavor at high- p_T

The cross-section of the Drell-Yan process $pp \rightarrow \ell_i^- \ell_j^+$ is given by

$$\sigma(pp \rightarrow \ell_i^- \ell_j^+) = \sum_{k,l} \int \frac{d\hat{s}}{s} \mathcal{L}_{q_k \bar{q}_l} \hat{\sigma}(q_k \bar{q}_l \rightarrow \ell_i^- \ell_j^+), \quad (2)$$

with

$$\mathcal{L}_{q_k \bar{q}_l}(\hat{s}) \equiv \int_{\hat{s}/s}^1 \frac{dx}{x} \left[f_{q_k}(x, \mu_F) f_{\bar{q}_l}\left(\frac{\hat{s}}{sx}, \mu_F\right) + (q_k \leftrightarrow \bar{q}_l) \right], \quad (3)$$

where $\sqrt{s} = 13$ TeV, i, j and k, l stand for lepton and quark flavor indices, respectively, f_{q_k} and $f_{\bar{q}_l}$ denote the Parton Distribution Functions (PDFs) of q_k and \bar{q}_l , and μ_F is the factorization scale. The partonic cross-section $\hat{\sigma}(q_k \bar{q}_l \rightarrow \ell_i^- \ell_j^+)$ contains the SM contributions, as well as the ones induced by higher-dimensional operators, as computed e.g. in Ref. [6]. The energy enhancement of the cross-section can compensate to some extent the heavy-flavor PDF suppression, thus allowing us to probe the five quark flavors available in the proton. Furthermore, LHC also allows probing

quark-flavor violating processes (with $q \neq l$), such as the $b \rightarrow s$ transition, if they are induced by $d = 6$ operators.

We consider the reinterpretation of the available CMS and ATLAS searches for the dilepton $pp \rightarrow \ell\ell'$ and monolepton $pp \rightarrow \ell\nu$ channels at high- p_T from Ref. [7], with 140 fb^{-1} . These results cover all possible leptons in the final state and they are implemented in the HighPT package.¹

4. Explicit examples

4.1 $b \rightarrow c\tau\nu$

Current status: The first example that we consider to discuss the complementarity of low- and high-energy searches is the $b \rightarrow c\tau\nu$ transition. Lepton Flavor Universality (LFU) ratios based on the $b \rightarrow c\ell\bar{\nu}$ transition have been determined to be [9]

$$R_D^{\text{exp}} = \frac{\mathcal{B}(B \rightarrow D\tau\nu)}{\mathcal{B}(B \rightarrow D\ell\nu)} = 0.357(29), \quad R_{D^*}^{\text{exp}} = \frac{\mathcal{B}(B \rightarrow D^*\tau\nu)}{\mathcal{B}(B \rightarrow D^*\ell\nu)} = 0.284(12), \quad (4)$$

which are larger than the SM predictions, $R_D^{\text{SM}} = 0.294(4)$ [10] and $R_{D^*}^{\text{SM}} = 0.265(13)$ [11] (see also Ref. [13]). While there is an agreement for the $B \rightarrow D$ transition between different lattice QCD determinations [12], there is still an ongoing debate for the different calculations of $B \rightarrow D^*$ form-factors [11, 13] and their compatibility with $B \rightarrow D^*\ell\nu$ differential data [9]. This issue is particularly important for the determination of $|V_{cb}|$ from $B \rightarrow D^*\ell\nu$, which is considerably lower than the inclusive determinations.

Before discussing the interpretations of these experimental results, we emphasize that the definition of the $B \rightarrow D^{(*)}$ LFU ratios could be optimized to reduce the impact of theoretical uncertainties. This could be achieved by defining observables where the (known) LFU-breaking effects from the SM are already taken into account. These definitions can be particularly useful for $B \rightarrow D^*$, where the various form-factor determinations disagree [14, 15]:

- Firstly, a very simple but useful modification that already allows to reduce the theoretical uncertainties is to consider the same bins in the denominator and numerator, i.e. $q^2 \in [m_\tau^2, (m_B - m_{D^{(*)}})^2]$, defining R_D^{cut} [14, 15]. For this observable, we obtain slightly more precise SM predictions, namely $R_D^{\text{cut}} = 0.572(4)$ and $R_{D^*}^{\text{cut}} = 0.343(6)$, for the same form-factors, which reduce the SM uncertainties by a factor of ≈ 2 in both cases.
- In the case of $B \rightarrow D^*$ decays, the LFU ratio can be further optimized by reweighing the muon rates as follows [15],²

$$R_{D^{(*)}}^{\text{opt}} = \frac{\int_{m_\tau^2}^{q_{\text{max}}^2} dq^2 \frac{d\mathcal{B}}{dq^2}(B \rightarrow D^{(*)}\tau\bar{\nu})}{\int_{m_\tau^2}^{q_{\text{max}}^2} dq^2 \left[\frac{\omega_\tau(q^2)}{\omega_\mu(q^2)} \right] \frac{d\mathcal{B}}{dq^2}(B \rightarrow D^{(*)}\mu\bar{\nu})}, \quad (5)$$

¹<https://github.com/HighPT>

²Note that such a cancellation would not be efficient for $B \rightarrow D$ decays, since the scalar form-factor (f_0) contribution is sizable, appearing with a different phase-space prefactor.

where $\omega_\ell(q^2) \equiv (1 - m_\ell^2/q^2)^2(1 + m_\ell^2/2q^2)$ is the lepton-dependent part of the phase-space function. In this case, we find $R_{D^*}^{\text{opt}} = 1.080(4)$, which improves the relative precision by a factor of ≈ 10 in comparison to the usual definition. Notice that the above definitions only require a redefinition of the muon rates, for which the differential spectrum can be easily binned, as already performed at the B -factories [9].

Even though the experimental uncertainties are still dominant, having more precise SM predictions will be needed, given the expected sensitivity of Belle-II for these observables [16].

Low- vs high-energy probes The most general effective Lagrangian describing the $b \rightarrow c\tau\bar{\nu}$ with operators up to $d = 6$ reads

$$\begin{aligned} \mathcal{L}_{\text{eff}}^{b \rightarrow c\tau\nu} = & -2\sqrt{2}G_F V_{cb} \left[(1 + C_{V_L})(\bar{c}_L \gamma_\mu b_L)(\bar{\tau}_L \gamma_\mu \nu_L) + C_{V_R}(\bar{c}_R \gamma_\mu b_R)(\bar{\tau}_L \gamma_\mu \nu_L) \right. \\ & \left. + C_{S_L}(\bar{c}_R b_L)(\bar{\tau}_R \nu_L) + C_{S_R}(\bar{c}_L b_R)(\bar{\tau}_R \nu_L) + C_T(\bar{c}_R \sigma_{\mu\nu} b_L)(\bar{\tau}_R \sigma^{\mu\nu} \nu_L) \right] + \text{h.c.}, \end{aligned} \quad (6)$$

where $C_{V_{L(R)}}$, $C_{S_{L(R)}}$ and C_T are effective operators that can be matched onto the SMEFT ones from Table 1, see e.g. Ref. [7]. Several combinations of these effective coefficients can explain current data, as discussed e.g. in Ref. [17]. One of the simplest solutions of $R_{D^{(*)}}$ is to rescale the SM contribution via C_{V_L} , which receives contributions in the SMEFT from $C_{lq}^{(3)}$, with appropriate flavor indices. A possible ultraviolet completion of this scenario is the $U_1 \sim (\mathbf{3}, \mathbf{1}, 2/3)$ leptoquark, which induces $C_{lq}^{(1)} = C_{lq}^{(3)}$ [17]. The constraints from flavor, electroweak precision and Drell-Yan data on these coefficients are shown in Fig. 1 for both the EFT and the U_1 leptoquark. Clearly, there is a complementarity of these different probes. Similar conclusions hold for the other SMEFT operators contributing to $b \rightarrow c\tau\nu$ such as C_{ledq} , $C_{lequ}^{(1)}$ and $C_{lequ}^{(3)}$, as discussed in detail in Ref. [7].

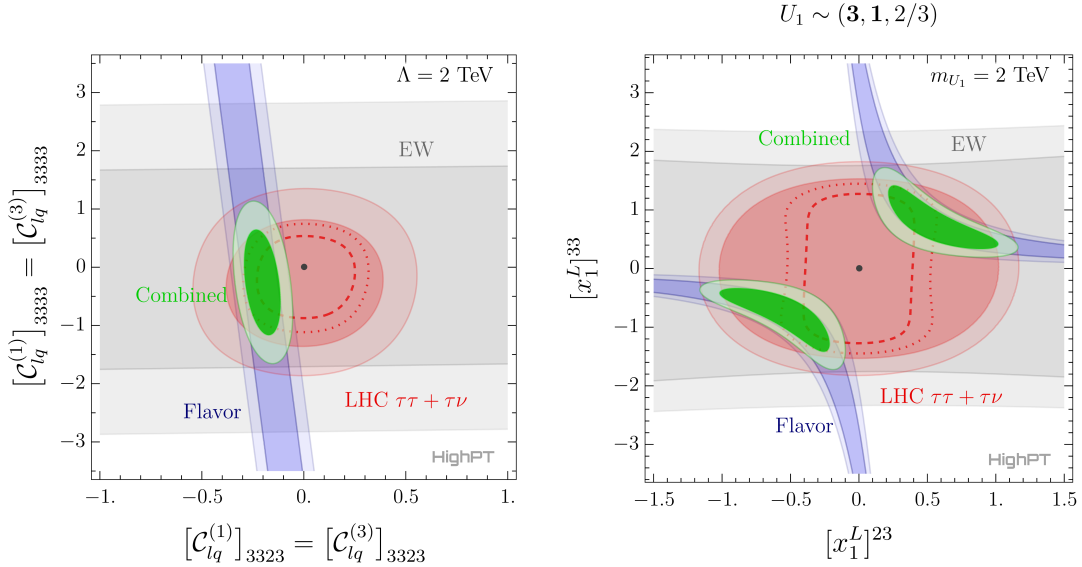


Figure 1: Constraints on the SMEFT coefficients (left panel) and the corresponding U_1 leptoquark couplings (right panel from flavor-physics (blue region), electroweak-precision (gray) and high- p_T LHC observables (red)). The combined fit is shown in green. See Ref. [7] for details.

4.2 $b \rightarrow s\nu\bar{\nu}$

Current status Another powerful probe of new physics are the theoretically clean decays $B \rightarrow K^{(*)}\nu\bar{\nu}$ [18], which are currently being studied at the Belle-II experiment. The current experimental values read [19, 20]

$$\mathcal{B}(B^+ \rightarrow K^+\nu\bar{\nu})^{\text{exp}} = 2.40(67) \times 10^{-5}, \quad \mathcal{B}(B^0 \rightarrow K^{*0}\nu\bar{\nu})^{\text{exp}} < 2.7 \times 10^{-5} \text{ (90\% CL)}, \quad (7)$$

which are to be compared to the SM predictions, $\mathcal{B}(B \rightarrow K\nu\bar{\nu})^{\text{SM}} = (4.44 \pm 0.14 \pm 0.27) \times 10^{-6}$ and $\mathcal{B}(B \rightarrow K^*\nu\bar{\nu})^{\text{SM}} = (9.05 \pm 1.25 \pm 0.55) \times 10^{-6}$, where the first uncertainty corresponds to the form-factors and the second one to the CKM elements, see Ref. [21] for a detailed discussion on the theoretical inputs. Note, in particular, that the $\mathcal{B}(B \rightarrow K\nu\bar{\nu})$ value obtained by the recent Belle-II measurement is considerably above its SM value [22].

Low- vs. high-energy probes The effective Lagrangian describing the $b \rightarrow s\nu\bar{\nu}$ transition with operators up to $d = 6$ reads

$$\mathcal{L}_{\text{eff}}^{b \rightarrow s\nu\bar{\nu}} = \frac{8G_F}{\sqrt{2}} \frac{\alpha_{\text{em}}}{4\pi} \sum_{i,j} \left[C_L^{ij} (\bar{s}_L \gamma^\mu b_L) (\bar{\nu}_{Li} \gamma_\mu \nu_{Lj}) + C_R^{ij} (\bar{s}_R \gamma^\mu b_R) (\bar{\nu}_{Li} \gamma_\mu \nu_{Lj}) \right] + \text{h.c.}, \quad (8)$$

where i, j are the neutrino flavor indices and $C_{L(R)}^{ij}$ are the Wilson coefficients. In the SM, only $C_L^{ij} = C_L^{\text{SM}} \delta^{ij}$ is nonzero, with $C_L^{\text{SM}} = -6.32(7)$ [18]. The C_L and C_R effective coefficients receive tree-level contributions from $C_{lq}^{(1,3)}$ and C_{ld} [18], respectively.

Even though there is not a precise LHC observable that can efficiently probe the $b \rightarrow s\nu\bar{\nu}$ transition at high- p_T , it should be stressed that the SMEFT operators contributing to $b \rightarrow s\nu\bar{\nu}$ will also contribute e.g. to $b\bar{s} \rightarrow \ell\bar{\ell}$ and $b\bar{c} \rightarrow \ell\nu$, which can be probed at high- p_T [6]. To illustrate this complementarity, we consider two SMEFT scenarios depicted in Fig. 2: (i) $C_{lq}^{(1)} = -C_{lq}^{(3)}$ vs. $C_{lq}^{(1)} = +C_{lq}^{(3)}$, and (ii) $C_{lq}^{(1)} = -C_{lq}^{(3)}$ vs. C_{ld} , with the quark flavor indices corresponding to the $b \rightarrow s$ transition and the leptonic to the τ -lepton.³ We find that right-handed operators are preferred to explain the excess in the $B^+ \rightarrow K^+\nu\bar{\nu}$ results [22]. Furthermore, we find once again that low- and high-energy are complementary in probing the SMEFT operators.

5. Summary

By using the results from Ref. [6, 7], we have shown in two explicit examples that Drell-Yan constraints on SMEFT operators relevant for B -physics can be complementary to low-energy measurements of tree- and loop-induced B -meson decays. Similar studies have also been made for the charm sector in Ref. [23] and for LFV decays in Ref. [24]. These examples illustrate that the combination of low- and high-energy searches is fundamental in order to understand discrepancies in low-energy observables, such as $R_{D^{(*)}}$, and to constrain the possible flavor structure of physics beyond the SM.

Acknowledgment

This project has received support from the European Union's Horizon 2020 research and innovation programme under the Marie Skłodowska-Curie grant agreement No 860881-HIDDeN.

³We focus on the τ -lepton as the couplings to electrons and muons are already tightly constrained, cf. Ref. [22].

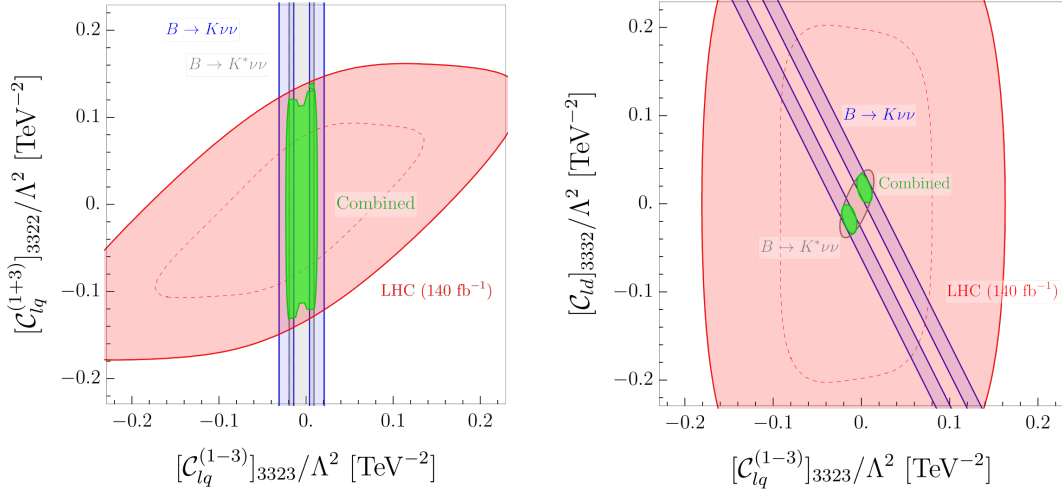


Figure 2: Low- and high-energy constraints on the SMEFT coefficients coupled to left-handed τ -leptons that are relevant to the $b \rightarrow sv\bar{\nu}$ transition. In the left panel, flavor and LHC constraints are complementary. In the right panel, flavor constraints are far more constraining. We use the shorthand notation $C_{lq}^{(1\pm 3)} \equiv C_{lq}^{(1)} \pm C_{lq}^{(3)}$.

References

- [1] G. Isidori, Y. Nir and G. Perez, *Ann. Rev. Nucl. Part. Sci.* **60** (2010), 355 [arXiv:1002.0900 [hep-ph]].
- [2] R. K. Ellis, B. Heinemann, J. de Blas, M. Cepeda, C. Grojean, F. Maltoni, A. Nisati, E. Petit, R. Rattazzi and W. Verkerke, *et al.* [arXiv:1910.11775 [hep-ex]].
- [3] G. D’Ambrosio, G. F. Giudice, G. Isidori and A. Strumia, *Nucl. Phys. B* **645** (2002), 155-187 [arXiv:hep-ph/0207036 [hep-ph]].
- [4] R. Barbieri, G. Isidori, J. Jones-Perez, P. Lodone and D. M. Straub, *Eur. Phys. J. C* **71** (2011), 1725 [arXiv:1105.2296 [hep-ph]].
- [5] B. Grzadkowski, M. Iskrzynski, M. Misiak and J. Rosiek, *JHEP* **10** (2010), 085 [arXiv:1008.4884 [hep-ph]]; W. Buchmuller and D. Wyler, *Nucl. Phys. B* **268** (1986), 621-653
- [6] L. Allwicher, D. A. Faroughy, F. Jaffredo, O. Sumensari and F. Wilsch, *JHEP* **03** (2023), 064 [arXiv:2207.10714 [hep-ph]].
- [7] L. Allwicher, D. A. Faroughy, F. Jaffredo, O. Sumensari and F. Wilsch, high- p_T Drell-Yan tails beyond the standard model,” *Comput. Phys. Commun.* **289** (2023), 108749 [arXiv:2207.10756 [hep-ph]].
- [8] M. Farina, G. Panico, D. Pappadopulo, J. T. Ruderman, R. Torre and A. Wulzer, *Phys. Lett. B* **772** (2017), 210-215 [arXiv:1609.08157 [hep-ph]].
- [9] Y. S. Amhis *et al.* [HFLAV], *Phys. Rev. D* **107** (2023) no.5, 052008 [arXiv:2206.07501 [hep-ex]].

- [10] Y. Aoki *et al.* [Flavour Lattice Averaging Group (FLAG)], *Eur. Phys. J. C* **82** (2022) no.10, 869 [arXiv:2111.09849 [hep-lat]].
- [11] A. Bazavov *et al.* [Fermilab Lattice, MILC, Fermilab Lattice and MILC], *Eur. Phys. J. C* **82** (2022) no.12, 1141 [erratum: *Eur. Phys. J. C* **83** (2023) no.1, 21] [arXiv:2105.14019 [hep-lat]].
- [12] H. Na *et al.* [HPQCD], *Phys. Rev. D* **92** (2015) no.5, 054510 [erratum: *Phys. Rev. D* **93** (2016) no.11, 119906] [arXiv:1505.03925 [hep-lat]] J. A. Bailey *et al.* [MILC], *Phys. Rev. D* **92** (2015) no.3, 034506 [arXiv:1503.07237 [hep-lat]].
- [13] J. Harrison and C. T. H. Davies, [arXiv:2304.03137 [hep-lat]]; Y. Aoki *et al.* [JLQCD], [arXiv:2306.05657 [hep-lat]].
- [14] M. Freytsis, Z. Ligeti and J. T. Ruderman, *Phys. Rev. D* **92** (2015) no.5, 054018 [arXiv:1506.08896 [hep-ph]].
- [15] G. Isidori and O. Sumensari, *Eur. Phys. J. C* **80** (2020) no.11, 1078 [arXiv:2007.08481 [hep-ph]].
- [16] E. Kou *et al.* [Belle-II], *PTEP* **2019** (2019) no.12, 123C01 [erratum: *PTEP* **2020** (2020) no.2, 029201] [arXiv:1808.10567 [hep-ex]].
- [17] A. Angelescu, D. Bečirević, D. A. Faroughy, F. Jaffredo and O. Sumensari, *Phys. Rev. D* **104** (2021) no.5, 055017 [arXiv:2103.12504 [hep-ph]]; C. Cornella, J. Fuentes-Martin and G. Isidori, *JHEP* **07** (2019), 168 [arXiv:1903.11517 [hep-ph]]; D. Buttazzo, A. Greljo, G. Isidori and D. Marzocca, *JHEP* **11** (2017), 044 [arXiv:1706.07808 [hep-ph]].
- [18] A. J. Buras, J. Girrbach-Noe, C. Niehoff and D. M. Straub, *JHEP* **02** (2015), 184 [arXiv:1409.4557 [hep-ph]]; J. Brod, M. Gorbahn and E. Stamou, *Phys. Rev. D* **83** (2011), 034030 [arXiv:1009.0947 [hep-ph]].
- [19] J. Grygier *et al.* [Belle], *Phys. Rev. D* **96** (2017) no.9, 091101 [arXiv:1702.03224 [hep-ex]].
- [20] A. Glazov, plenary talk given at the EPS-HEP2023 Conference in Hamburg (Germany), Aug 20-25, 2023.
- [21] D. Bečirević, G. Piazza and O. Sumensari, *Eur. Phys. J. C* **83** (2023) no.3, 252 [arXiv:2301.06990 [hep-ph]].
- [22] R. Bause, H. Gisbert and G. Hiller, [arXiv:2309.00075 [hep-ph]]; L. Allwicher, D. Becirevic, G. Piazza, S. Rosauero-Alcaraz and O. Sumensari, [arXiv:2309.02246 [hep-ph]].
- [23] J. Fuentes-Martin, A. Greljo, J. Martin Camalich and J. D. Ruiz-Alvarez, *JHEP* **11** (2020), 080 [arXiv:2003.12421 [hep-ph]].
- [24] A. Angelescu, D. A. Faroughy and O. Sumensari, *Eur. Phys. J. C* **80** (2020) no.7, 641 [arXiv:2002.05684 [hep-ph]]; S. Descotes-Genon, D. A. Faroughy, I. Plakias and O. Sumensari, *Eur. Phys. J. C* **83** (2023) no.8, 753 [arXiv:2303.07521 [hep-ph]].